ELSEVIER

Journal of Photochemistry and Photobiology A: Chemistry 131 (2000) 111–123

Journal of Photochemistry and Photobiology A:Chemistry

www.elsevier.nl/locate/jphotochem

Anion effect in linear silver nanoparticle aggregation as evidenced by efficient fluorescence quenching and SERS enhancement

Swati De [a], Anjali Pal [b], Nikhil Ranjan Jana [c], Tarasankar Pal [d,*]

[a] *Department of Chemistry, Kalyani University, Nadia, India*

[b] *Civil Engineering Department, Indian Institute of Technology, Kharagpur 721302, India*

[c] *Raja Rammohun Mahavidyalaya, Hooghly, India*

[d] *Department of Chemistry, Indian Institute of Technology, Kharagpur 721302, India*

Received 6 August 1999; received in revised form 1 November 1999; accepted 20 November 1999

Abstract

This work is the first report of the effect of anions of precursor salts on the efficiency of photochemical reduction of Ag (I) to Ag (0). Ultraviolet (UV) irradiation of an aqueous Triton X-100 solution in the presence of Ag (I) produces the green sol at a certain critical concentration of ascorbic acid. The photochemical process of silver sol formation possesses the advantage of producing homogeneous particles of very small size (~6 nm). In the presence of a reduction sensitizer, such as ascorbic acid, these tiny silver dots aggregate beautifully in a symmetric manner to form necklace-like structures. Fluorescence quenching studies carried out with the probe 1-aminonaphthalene give an idea about the structure and binding capacities of the sols, the latter effect being more pronounced for the linearly aggregated sol. Fluorescence and AFM studies complimented by surface-enhanced Raman scattering (SERS) studies with pyridine reveal that the green silver sol consists of linear aggregates, whereas the yellow sol does not contain the aggregated arrangement. The most interesting result arising out of this study is that linear aggregation of spherical silver sols leads to enhanced efficiency as fluorescence quenchers as also an improvement in SERS activity. These linear aggregates of silver may hold prospects for the development of interconnecting quantum devices in future.

Keywords: 1-Aminonaphthalene (1-AN); Fluorescence; SERS; Colloids; UV irradiation

1. Introduction

Colloids comprise suspensions of one phase in another. Recent years have seen a widespread interest in the structure and reactivity of transition metal colloids [1]. Metal nanoclusters have close-lying conduction and valence bands and thus, electrons move about freely. The free electrons give rise to a surface plasmon absorption band, which depends on both the cluster size and chemical surroundings [2–4]. Thus, the colors of the colloids vary depending on the method of preparation and the state of aggregation. Silver colloids are widely studied because of their applicability in surface-enhanced Raman scattering (SERS) [5–10] and their use in the photographic process [11,12]. Prolate spheroids and bispherical particles are particularly effective in SERS [13–16]. The net effect of deviation from the spherical shape is splitting of the dipole resonance into two absorption bands, in which the induced dipole oscillates along and transverse to the spheroidal axis. In the longitudinal resonance, the band increases in cross-section and shifts to longer wavelengths. In the transverse resonance, the band remains more or less intact [6]. The change-over from spherical to ellipsoidal shape results in shifting the absorption into the UV–VIS range [17]. The appearance of a new peak at a longer wavelength region is often ascribed to the formation of loosely-packed aggregates [3,4,34,35]. The latter are formed due to dipole interaction between neighboring particles. The optical properties of Ag colloids depend not only on the size and shape of the particles but also on the change in electron density on their surface [13–16,18–22].

The present study reports on the photochemical reduction of Ag (I) to produce silver sols and the effect of various additives on this process. Comparison is also made with similar effects on the chemical reduction of Ag (I). Further, the effect of Ag sols on various photo-processes, such as fluorescence and SERS, have been studied with a view to correlate structural and size-related effects.

The effect of Ag sols on fluorescence was studied using the well-known fluorophore, 1-aminonaphthalene (1-AN). Ag colloids and island films are known to quench the

* Corresponding author.

1010-6030/00/$ – see front matter
PII: S1010-6030(99)00231-2

fluorescence of organic fluorophores [23–25]. Recently, Tata et al. have observed fluorescence quenching due to CdS nanoparticles by thiol-containing compounds in the Aerosol-OT (AOT) water-in-oil microemulsions [26]. The choice of 1-AN as the fluorophore was mainly due to its widely studied fluorescence properties and secondly due to its high quantum yield (ϕ_f=0.5) [27,28]. The fluorescent state of 1-AN in polar solvents has significant charge transfer character [27,28]. Thus, the fluorescence of 1-AN is susceptible to changes in its immediate surroundings.

Fluorescence quenching induced by colloidal metals and other such particles is much higher than the well-known 'heavy atom effect' [25,29,30]. Weitz et al. proposed a model for colloid-induced fluorescence quenching describing the effect of electronic plasma resonance on the light scattering process [23].

Since Fleischmann et al. [31] first reported SERS of pyridine adsorbed on a Ag electrode, there have been various studies on this phenomenon. SERS on the surface of colloidal particles is attributed to two mechanisms: (1) the resonant enhancement of the electromagnetic field close to the metal surface when the incident light lies within an absorption band of the colloidal particles; (2) resonance enhancement of the Raman scattering tensor for the molecules adsorbed at the surface due to scattering close to the metal-adsorbate charge-transfer (CT) transitions. The first is the electromagnetic effect and the second is the chemical effect. The predominant view regarding SERS is that the major contribution is electromagnetic. Hence the λ_{max}^{abs} of the colloidal particles corresponds approximately to the most efficient excitation wavelength for SERS [6].

2. Experimental section

All salts, acids, alkalis and other chemicals used were AR grade. Water distilled twice over $KMnO_4$ was used for the experiments. The non-aqueous solvents used, that is benzene and *n*-hexane (all spectroscopic grade) were first dried over metallic sodium and then distilled. Poly (oxyethylene) *iso*-octylphenyl ether (TX-100) obtained from Fluka and used for the preparation of reverse micelles was purified following literature procedures [32]. $AgClO_4$ and $LiClO_4$ were prepared in the laboratory. $LiClO_4$ was prepared by adding Li_2CO_3 (99%) to perchloric acid contained in a water, bath maintained at 60°C. Once the brisk effervescence ceased, the contents were filtered and the precipitate of $LiClO_4$ obtained by evaporating water was washed and dried. $AgClO_4$ was prepared by passing $AgNO_3$ through an anion-exchange resin (AER) previously soaked in 5N $HClO_4$.

Reverse micelles were prepared from 0.3 M TX-100 in 30% (v/v) benzene and 70% (v/v) *n*-hexane. Microliter amounts of an aqueous solution of Ag_2SO_4 (1×10^{-2} M) were added into the reverse micelle. The resulting mixture was shaken well so as to get a clear solution. To this, microliter amounts of an aqueous solution of ascorbic acid (AA, 56.8 mM) were added. The total amount of water added was controlled so as to obtain the desired ratio w_0, that is, $[H_2O]/[TX\text{-}100]$ ratio.

For UV irradiation, a TUV 15 W G15T8 lamp supplied by Philips (India) was used. The sample was taken in a 1 cm quartz cuvette and exposed to UV radiation at a distance of 8 cm from the lamp. The irradiation time for all the experiments was 10 min. UV–VIS absorption spectra were measured in a Shimadzu UV-160 digital spectrophotometer (Kyoto, Japan) with a 1 cm quartz cuvette.

The steady state fluorescence spectra were recorded in a Perkin–Elmer Luminoscope, Model LS 50B. Quantum yields (ϕ_f) were determined from the emission spectra using quinine sulfate (Q_2SO_4) in 0.5N H_2SO_4 (ϕ_f=0.55) as a standard. The wavelength of exciting light (λ_{ex}) was 320 nm. Fluorescence intensity decays were measured using the single-photon counting technique with an apparatus assembled from components of Edinburgh Instruments model 199F time-domain fluorometer. Excitation at 320 nm was provided by a pulsed high pressure nitrogen lamp operating at 25 kHz repetition rate and 1.5 atmosphere pressure, the pulse profile having a full-width at half maximum (FWHM) of 1.3 ns. The decay profiles were collected at 440 nm emission. Slit widths of 4 nm were used both in the excitation and emission channels. Lifetimes were estimated by fitting each individual profile to a single-exponential decay using supplied software.

The dynamic light scattering results were obtained with a Photal DLS-700 instrument supplied by Otsuka Electronics. The scattering angle was maintained at 90°. The scattering experiments were carried out at room temperature (27°C). SERS spectra were acquired with an instrument SA, HR-320 spectrograph equipped with Princeton instrument charged couple device (RE-ICCD). Measurements were done with Kr laser (200 mW) with 647.1 nm line and 30 μm entrance slit. All the spectra were single scans at a rate of 1 cm^{-1} sec^{-1}. Topographic images of Ag nanoparticles and nanostrings were obtained by tapping mode atomic force microscopy (TAFM) using Digital Instruments (Santa Barbara, USA). The size of the sols was estimated by allowing a tolerance limit for geometrical broadening arising due to the finite radius of the tip.

3. Results and discussion

3.1. General studies

3.1.1. Effect of different anions on extent of reduction of Ag (I)

Silver colloids were produced by the chemical reduction of different precursor salts. Using 2.5×10^{-4} M $NaBH_4$ as the reductant, the extent of reduction of 5×10^{-4} M of AgX (where X=NO_3^-, SO_4^{2-}) was found to be different for NO_3^- and SO_4^{2-}. In neat water, the band areas of the

absorption spectra (peaking at 400 nm) of the yellow colored silver sols prepared from Ag_2SO_4 and $AgNO_3$ were found to be in the ratio (R)∼3, where R=band area of absorption spectrum of silver sol prepared using Ag_2SO_4 as precursor/band area of absorption spectrum of silver sol prepared using $AgNO_3$ as precursor.

A similar difference was obtained using various stabilizers. For example, in gelatin R∼4, in TX-100 R∼2 and in β-cyclodextrin R∼2. On altering the reducing agent from $NaBH_4$ to AA, a similar difference was noted. The Ag particles being extremely small in size, there is a significant amount of scattering at the particle surfaces as a result of which there is a broadening of the absorption band. According to the Mie theory [10], the extent of absorption,

$$A = \frac{CN1}{2.303}$$

where C=absorption cross-section; N=number of particles; and l=path length.

Again, $C = k\varepsilon_2/\lambda[(\varepsilon_1 + 2)^2 + \varepsilon_2^2]$, where λ=incident wavelength; $\varepsilon=\varepsilon_1+i\varepsilon_2$, is the complex relative permittivity of the metal relative to the surrounding medium.

The width and height of the resonance is determined by ε_2.

Thus, the absorption cross-section and hence the extent of absorption is proportional to the bandwidth as also to peak height. Since for the chemically prepared yellow sol, there is a single absorption band peaking at 400 nm, the band area can be considered to be proportional to the number density of the unaggregated sol particles and hence to the extent of reduction of Ag (I) to Ag (0). Thus, differences in the extent of reduction of $AgNO_3$ and Ag_2SO_4 to Ag (0), under similar conditions exist. In order to probe further into the reason behind this difference, the photochemical reduction of Ag (I) to Ag (0) was studied using different precursor salts under the same experimental condition. Using 8.5×10^{-5} M AA to reduce 2.5×10^{-4} M AgX (where X=NO_3^-, SO_4^{2-}) R∼2 in presence of gelatin and 4 in presence of TX-100. The concentration of AgX was kept higher than that of the reducing agent AA so that complete stoichiometric reduction is not possible and hence the anion effect is more pronounced. However, with the addition of 0.5% (v/v) ethyl alcohol to TX-100, R decreased from 4 to 2. Moreover, it was found that in TX-100 medium or in TX/alcohol, addition of 8.5×10^{-5} M AA to 2.5×10^{-4} M $AgNO_3$ produced the characteristic yellow sol (with maximum absorption at λ_{max}^{abs}=400 nm). However, under similar conditions, 2.5×10^{-4} M Ag_2SO_4 produced a distinct green colored sol with a sharp peak at λ=400 nm and a broader peak of diminished intensity at λ=630 nm (Fig. 1). $AgNO_3$ also produced the green sol but at a higher concentration. The green sol was obtained only in the presence of a 1:1 TX-100/water medium.

On the basis of the above results, a systematic study was undertaken, in which three precursor salts: $AgNO_3$, $AgClO_4$ and Ag_2SO_4 were used to produce Ag colloids. One set of experiments comprised chemical reduction by $NaBH_4$ and the other set comprised photochemical reduction by AA. In both cases, aqueous TX-100 medium was used. Absorbance at 400 nm (in case of chemical reduction) and absorbances at both 400 nm and 630 nm (for photochemical reduction) were plotted versus the silver salt concentration [AgX] in mol l^{-1}. In each case, the plot obtained displayed a maximum for a certain AgX concentration (i.e. C^{max}). The behavior of the three different salts was compared using C^{max} as a criterion. In case of photochemical reduction by 8.5×10^{-5} M AA in 5×10^{-3} M TX-100, for absorbance monitored at 400 nm, C^{max} corresponding to Ag_2SO_4, $AgClO_4$ and $AgNO_3$ were 2.5×10^{-4}, 5×10^{-4} and 7.5×10^{-4} M, respectively (Fig. 2a). Again absorbance at 630 nm was monitored and C^{max} was 5×10^{-4} M for Ag_2SO_4, 1×10^{-3} M for $AgNO_3$ and 1.5×10^{-3} M for $AgClO_4$ (Fig. 2b). Since the total amount of Ag sols can be related to the absorbances at both 400 and 630 nm, it can be said that Ag_2SO_4 is a more efficient precursor for the formation of Ag sol as C^{max} corresponds to a lower concentration for Ag_2SO_4 compared to the other three salts. Moreover, in case of photochemical reduction, the green sol was also formed at much lower concentration for Ag_2SO_4 as compared to $AgClO_4$ and $AgNO_3$.

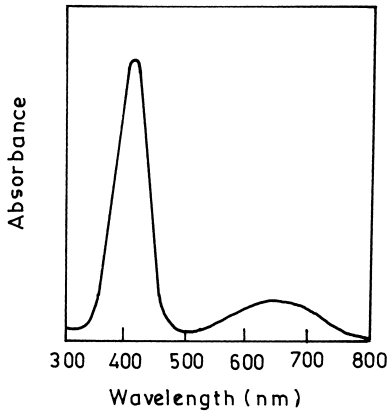

Fig. 1. Absorption spectra of the photochemically prepared green silver sols using Ag_2SO_4 as precursor. [Ag_2SO_4]=2.5×10^{-4} M; [TX-100]=5×10^{-3} M; [AA]=8.5×10^{-5} M.

The green Ag sol obtained in this work can be compared to the 'blue silver' reported in earlier studies [11,12,33,34]. Kamat et al. ascribed the visible band to a transient state, which is essentially an aggregate of small clusters and trapped electrons arising due to inter-particle changes [35]. It is known that aggregation of small Ag particles leads to a broad plasmon band in the visible region [2]. AFM studies on the green silver sols produced from Ag_2SO_4, $AgNO_3$ and $AgClO_4$ show the presence of linear aggregates each of diameter less than 6 nm. Although, the absorption spectra of the green sol (Fig. 1) shows the height of the 400 nm peak to be greater than that of the 630 nm peak, AFM results (Fig. 3) show that the green sol mainly consists of aggregated particles with a few scattered unaggregated particles. AFM studies of the yellow sol did not show the presence of linear aggregates as observed for the green sol.

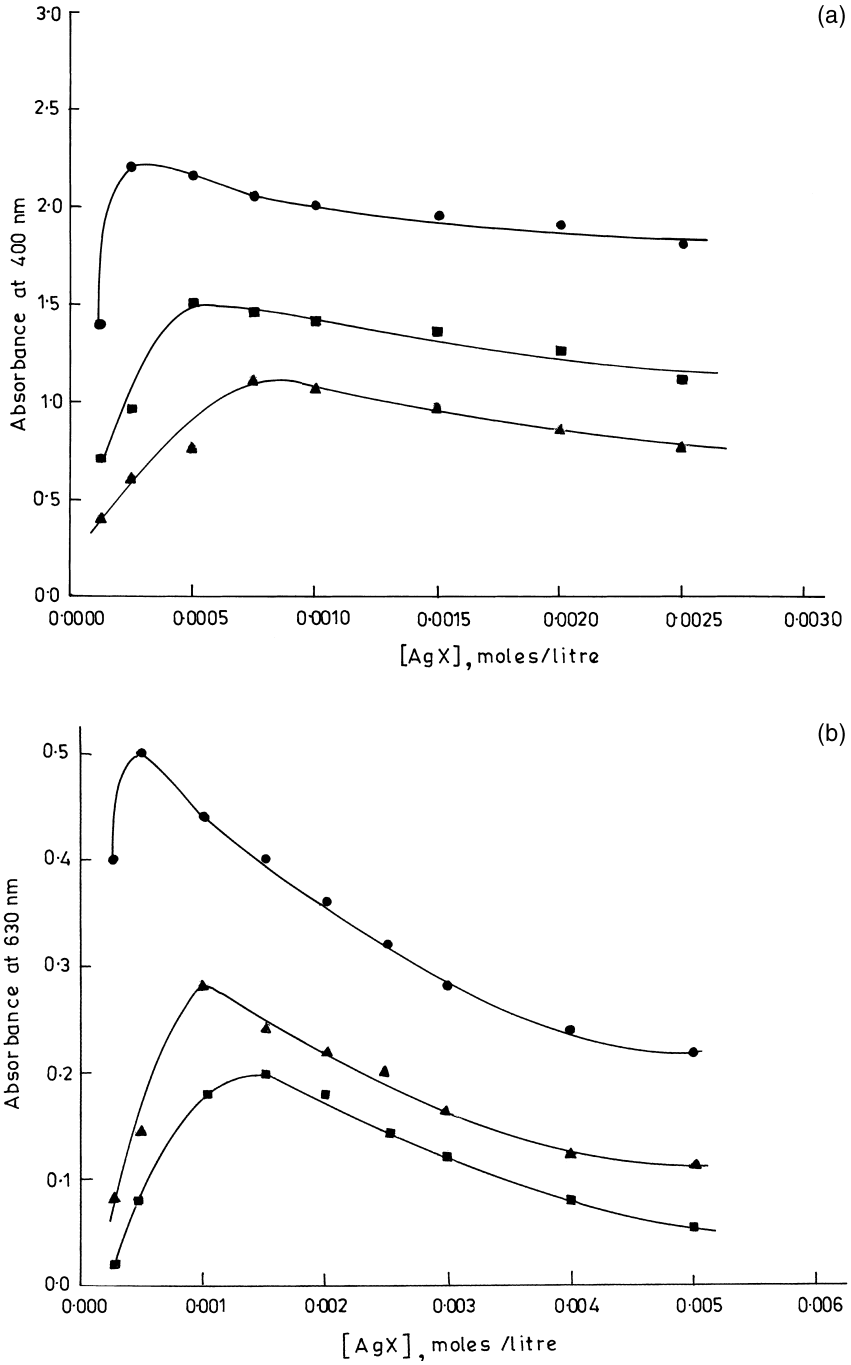

Fig. 2. Absorbance of the photochemically prepared silver sol plotted vs. Ag_2SO_4 (●), $AgNO_3$ (▲) and $AgClO_4$ (■) concentrations, [AA]=8.5×10^{-5} M, [TX-100]=5×10^{-3} M. Absorbance monitored at: (a) 400 nm and (b) 630 nm.

Following previous literature and from the AFM results, the green silver sol is ascribed to linear aggregates of individual particles. The chain propagation takes place through twin silver particle formation.

Dynamic light scattering (DLS) studies (Table 1) show that the photochemically prepared yellow silver sol has a mean diameter (d) of 24.4 nm, the chemically prepared yellow sol has d=26 nm and the photochemically prepared green sol has d=41.9 nm. All the sols were prepared from the same processor, that is $AgNO_3$. The apparent discrepancy between the d values obtained by AFM and DLS of the green sol can be attributed to the incorporation of the diameter of the micellar jacket surrounding the metal particle in case of DLS results. The green sol has the highest polydispersity, p.d.=0.9. The larger diameter of the green sol compared to the yellow one is an indication of the former being an aggregate. Another indicator of this fact is the higher diffusion coefficient of the yellow sol compared to

Table 1
Results of dynamic light scattering studies of various silver sols[a]

Type of sol studied	Diameter (nm)	Polydispersity	Diffusion coefficient ($cm^2\ s^{-1}$)
Photochemically prepared green silver sol	41.9	0.9	1.2×10^{-7}
Photochemically prepared yellow silver sol	24.4	0.7	2.1×10^{-7}
Chemically prepared yellow silver sol	26.0	0.4	2.0×10^{-7}

[a] Precursor salt used — $AgNO_3$; scattering angle — 90°; solvent viscosity — 0.84 cP; refractive index — 1.33.

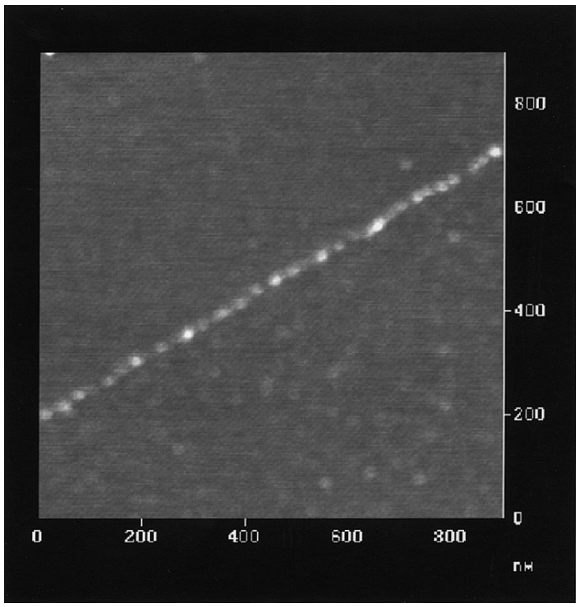

Fig. 3. AFM image of green silver sol.

the green one. The latter consisting of aggregated particles will diffuse slower than the yellow sol which consists of unaggregated particles. None of the autocorrelation functions fit perfectly with a single-exponential decay, the effect being more pronounced for the green sol. This would be due to polydispersity of the medium or existence of non-spherical particles, which can result from aggregation of individual spherical particles into random chains [7].

The effect of various anions can be explained as follows. The NO_3^- ion is a better electron scavenger than the SO_4^{2-} ion and hence the former can capture electrons released by the reducing agent [36]. Thus, lesser number of electrons are available for reducing Ag (I) and hence the silver plasmon band at 400 nm is diminished in intensity compared to that for SO_4^{2-}. Ag nanoparticles are known to undergo dissolution readily in presence of electron scavengers like N_2O [22]. Sulfate ions have been known to accelerate reduction of Ag (I) to the colloidal metal by specific adsorption on the particle surface [34]. The Ag (I) ion together with the electrical double layer forms a micelle type structure, which comprises a positively charged granule surrounded by an anionic layer. A characteristic of such an unstable system is the growth of the particles and hence reduction of the specific surface area. SO_4^{2-}, $HCOO^-$ and other such ions adsorb on the colloid surface. Thus, positive charge of the grain decreases leading to a compression of the electrical double layer. This leads to an increase in the coagulation rate of the Ag sol. Thus, the enhancement of the aggregate band at 630 nm in presence of SO_4^{2-} can be understood. On the other hand, ClO_4^- is inert relative to sorption on Ag sols [34,36]. In spite of this, it accelerates the formation of silver sols. The action of inert electrolytes too, proceeds via compression of the electrical double layer due to increase in ionic strength of the solution. However, SO_4^{2-} is most efficient in this respect as is obvious from a lower concentration of Ag_2SO_4 required for maximum absorbance at 630 nm compared to $AgClO_4$ and $AgNO_3$ (Fig. 2b). From the spectrochemical series, the ligating properties of all the three anions SO_4^{2-}, ClO_4^- and NO_3^- are almost comparable. However, SO_4^{2-} owing to its larger size is most effective in directing the silver sol system towards aggregation.

3.1.2. Effect of ascorbic acid

The concentration of the reductant, that is ascorbic acid (AA), has been found to be a deterministic factor in obtaining both the yellow and green Ag sols photochemically. The maximum absorbance at 630 nm for all the three precursor salts (i.e. $AgNO_3$, $AgClO_4$ and Ag_2SO_4) has been obtained at an AA concentration of 8.5×10^{-5} M (Fig. 4) and pH∼6. Below this critical concentration range, the yellow sol is obtained and above this a greenish cloudiness is seen in the solution. The next question that arises is regarding the mechanism by which AA reduces AgX in presence of UV light. Previous studies have used AA to reduce Ag salts but the reaction was usually carried out in alkaline media, that is the real reducing agent is the ascorbate anion (AA^-) not AA. In this report, however, neutral AA is the reducing species since the working pH is 6. To determine whether the reduction proceeds via a free radical mechanism, the reaction was performed under the same conditions with the additional presence of a radical inhibitor, hydroquinone (HQ). It was seen that under the same conditions, when the blank (i.e. sample without HQ) produces the green sol, a brown cloudiness is observed in the presence of HQ. However, in the presence of a radical initiator, that is benzoyl peroxide (BP), the characteristic green color is obtained. Thus, the photochemical reduction process may proceed via a radical mechanism.

The product formed from the reaction is dehydroascorbic acid (M^+=174) as evidenced from the GC-MS studies of the reaction mixture. This was followed by Norrish type of cleavage leading to mass fragments at *M*/*Z* 113, 95, 86, 60 and 59. The photochemical transformation of AA to dehydroascorbic acid in aqueous TX-100 medium in the presence

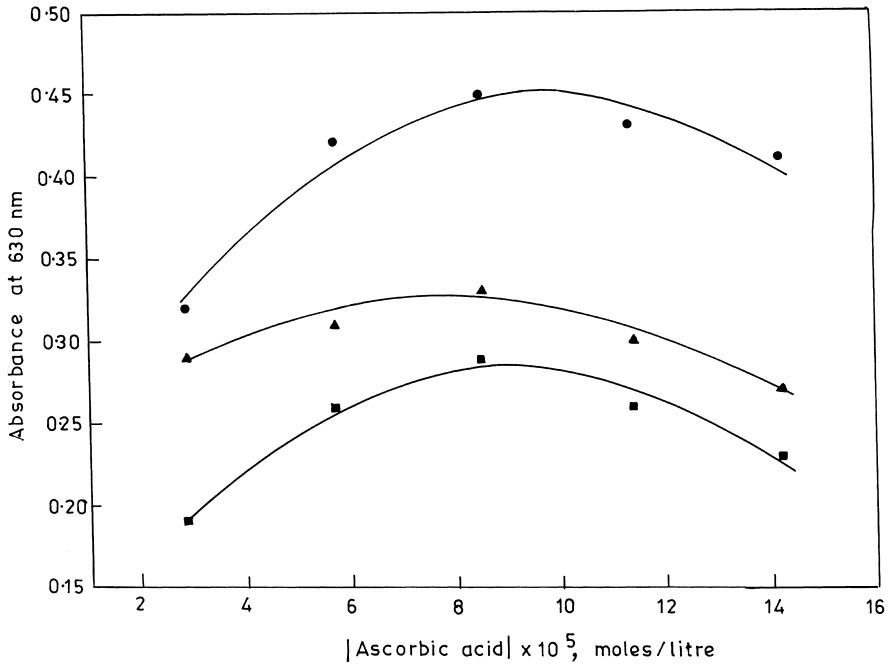

Fig. 4. Absorbance at 630 nm of the photochemically prepared green silver sol plotted vs. ascorbic acid concentration: (a)Ag_2SO_4 (●); (b) $AgNO_3$ (▲) and (c) $AgClO_4$ (■), [AgX]=2.5×10^{-4} M, [TX-100]=5×10^{-3}M.

of Ag (I), possibly follows a radical pathway. UV irradiation, may stimulate the photolysis of organic compounds, and thus give rise to reducing organic radicals [37].

However, although the photochemical reduction of Ag (I) may proceed, via a radical mechanism, examination of the ESR spectra of 'blue silver' shows the absence of radical species. Thus, the silver atoms are united into metallic clusters [34].

3.1.3. Effect of alcohol

Addition of 1% (v/v) EtOH to the reaction mixture undergoing photochemical reduction leads to increased absorbance at 630 nm in case of $AgNO_3$ and $AgClO_4$ precursors (Fig. 5). Alcohols produce highly reducing organic radicals. Thus, the net number of reducing species increases and hence a greater absorbance is likely to be observed. To test whether the increased absorbance at 630 nm

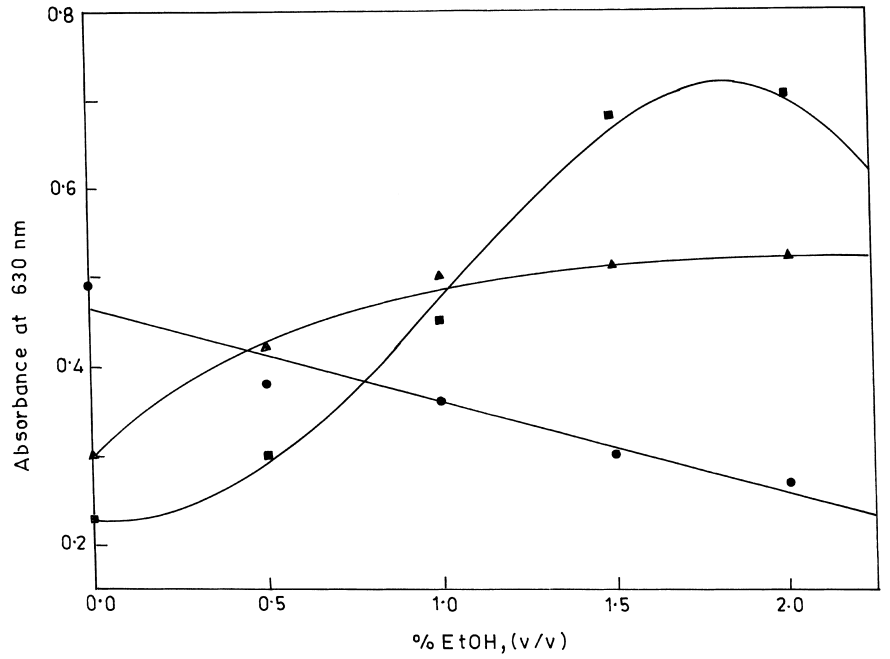

Fig. 5. Effect of alcohol on the green silver sol prepared from: (a) Ag_2SO_4 (●); (b) $AgNO_3$ (▲) and (c) $AgClO_4$ (■), [AgX]=2.5×10^{-4} M, [TX-100]=5×10^{-3} M, [AA]=8.5×10^{-5} M.

(in the presence of alcohol) is due to direct conversion of unaggregated particles into aggregated ones, 1% (v/v) EtOH was added to the yellow sol, which was then illuminated. No conversion of the yellow sol into green was observed. Thus, the alcohol effect can be ascribed to an increase in the amount of reducing species. This happens for ClO_4^- and NO_3^-. But for SO_4^{2-}, the decrease in absorbance with the addition of alcohol can be attributed to the displacement of the adsorbed SO_4^{2-} from the particle surface. This results in a decreased coagulation. The effect of alcohol can also be attributed to the changing dielectric constant of the medium. According to the Mie theory, the alcohol effect can be attributed to alteration in ε_2 value, which changes the absorbance [10].

3.1.4. Effect of added electrolyte

To test the effect of externally added electrolytes on the formation of the green sol, to 5×10^{-4} M AgX in 5×10^{-3} M TX-100 and 8.5×10^{-5} M AA, was added each of the salt solutions of KNO_3, $LiClO_4$ and Na_2SO_4. It was found that for each of the three precursor salts $AgNO_3$, $AgClO_4$ and Ag_2SO_4, addition of an electrolyte with a common anion leads to the largest increase in absorbance at 630 nm. Inert electrolytes lead to a smaller increase. With Ag_2SO_4 as the precursor salt, the absorbance at 630 nm was monitored versus the concentration variation of two externally added electrolytes: one with a common anion, that is Na_2SO_4 and another inert electrolyte, for example, $LiClO_4$. The results are plotted in Fig. 6. In both cases, the absorbance at 630 nm increases with the addition of the external electrolyte and reaches a maximum at an electrolyte concentration of 1×10^{-3} M, after which it decreases. However, the final values of absorbance are higher for Na_2SO_4 than $LiClO_4$. Thus, the addition of an external electrolyte facilitates the aggregation process. This fact has also been utilized for SERS studies reported later in this work.

3.1.5. Effect of other additives

Dilute ammonia causes lightening of the green color. NH_3 is an efficient complexing agent, which binds Ag (I) ions and carries them from the ion exchanger into the bulk of the solution. This decreases the number of Ag (I) ions within the linear clusters and thus decreases their stability. Addition of solid iodine leads to instant discharging of both the yellow and green colors [29], while solid KI discharges the green color to yield a yellow color. The adsorption of I^- on the particle surface is known to alter the surface plasmon band [21].

In order to test whether the yellow sol can be transformed to the green sol, excess Na_2SO_4 was added to the former and the mixture was then irradiated. No change in the yellow color was observed, thus showing that yellow to green transformation is not possible by the mere addition of electrolyte, although the reversed transformation is easily achieved. Addition of dilute HCl to the green sol resulted in its conversion into the yellow sol while dilute NaOH led to a blackish coloration. Thus, highly acidic and highly alkaline media hinder the formation of green sol and an optimum pH of 6 is most suitable.

3.1.6. Effect of an anion exchange resin on the green colloid

To the activated anion-exchange resin (Amberlite IRA-400), the green sol prepared from Ag_2SO_4 was added.

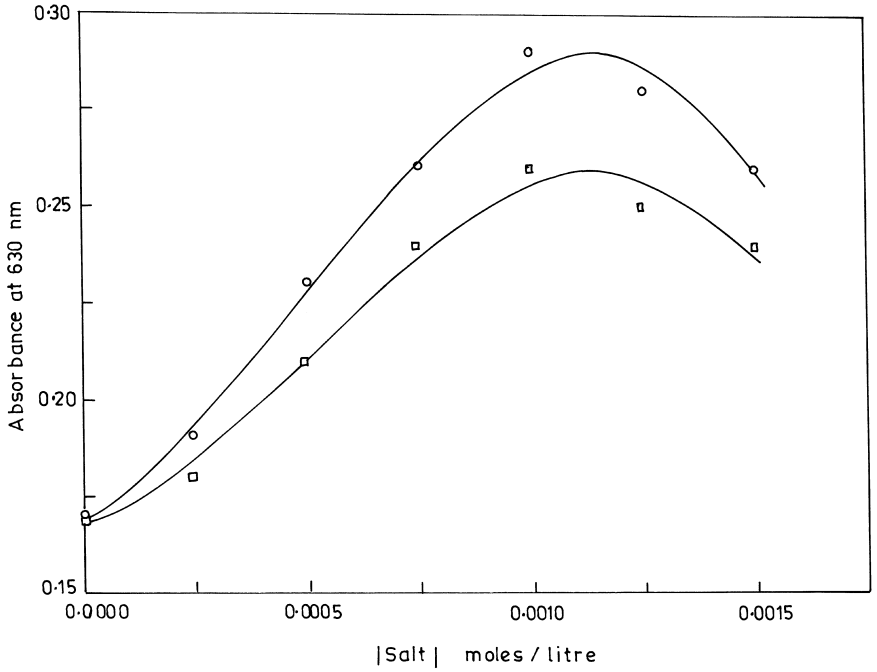

Fig. 6. Effect of externally added electrolyte on the formation of green sol using Ag_2SO_4 as precursor: (a) Na_2SO_4 (○) and (b) $LiClO_4$ (□), $[Ag_2SO_4]=5\times10^{-4}$ M, $[TX\text{-}100]=5\times10^{-3}$ M, $[AA]=8.5\times10^{-5}$ M.

Table 2
UV–VIS absorption studies in reverse micelles of TX-100 in benzene/*n*-hexane (30:70%)[a]

w_0=[H_2O]/[TX-100]	[Ag_2SO_4] in mol l^{-1}	[Ascorbic acid] in mol l^{-1}	Absorbance at 400 nm
0.5	1.5×10^{-5}	5.7×10^{-5}	0.2
1.0	3.9×10^{-5}	5.7×10^{-5}	0.3
1.5	6.3×10^{-5}	5.7×10^{-5}	0.5
2.0	8.7×10^{-5}	5.7×10^{-5}	0.8
2.5	11.2×10^{-5}	5.7×10^{-5}	1.0
4.0	18.5×10^{-5}	5.7×10^{-5}	2.2

[a] [TX-100]=0.3 M.

The green color was found to slowly fade, finally yielding a yellow coloration. The resin was then tested for adsorbed SO_4^{2-}. $BaCl_2$ solution in contact with the resin showed signs of turbidity thus proving that the resin removes SO_4^{2-} from the green sol. This is an indirect proof that the presence of SO_4^{2-} is essential for the existence of the aggregated Ag sol.

3.1.7. Reduction in reverse micelles

There are previous reports of preparation of Ag sols in AOT reverse micelles [38]. The aim of this work was to prepare Ag sols in reverse micelles by UV irradiation. However, addition of AA to $AgNO_3$ solubilized in the water pools of TX-100 reverse micelles led to instantaneous formation of the yellow sol. Further irradiation led to no perceptible change. The results are summarized in Table 2. However, phase separation occurred beyond $w_0\sim5$. The instant development of yellow color in reverse micelles may be due to the higher surface pH on the reverse micellar surface. The interesting observation from this study is the fact that the same surfactant, that is TX-100 sometimes promotes the formation of aggregated green sol (when it forms normal micelles) and sometimes fails to form the aggregated sol (i.e. when it form reverse micelles). The reason for this may be that the minute water pools within the reverse micelles impede the process of aggregation by encapsulating individual particles and shielding them from neighboring particles by means of the surfactant layer surrounding the individual water pools. Thus, the open environment found in normal micelles is conducive to the process of particle aggregation. Another important observation is that TX-100 with its polymer-like structure promotes the formation of aggregates, whereas other surfactants like the cationic cetyl trimethyl ammonium bromide (CTAB) and the anionic sodium dodecyl sulfate (SDS) fail to induce aggregation of Ag particles. For, TX-100 also, in an open polymeric configuration as in normal micelles, can induce aggregation, while in the confined region of reverse micelles, it fails to do so.

3.2. Fluorescence studies

The absorption and emission spectra of 2.5×10^{-5} M 1-AN were studied in 4×10^{-3} M aqueous TX-100. The TX-100 concentration is maintained well over its critical micellar concentration (CMC). The emission characteristics are summarized in Table 3. The absorption maxima, λ_{max}^{abs} of 1-AN in aqueous TX-100 is at 315 nm. The fluorescence peak in aqueous TX-100 is at 440 nm, which is blue, shifted compared to that in neat water [27,28]. The absolute quantum yields (ϕ_f) determined with respect to Q_2SO_4 as standard are listed in Table 3. ϕ_f of 1-AN in neat water was found to be 0.46 at pH=6. This value is consistent with literature values [27]. However, on being incorporated into TX-100 micelles, the ϕ_f of 1-AN increases to 0.6. This increase in ϕ_f is probably due to a decrease in the rate of excited-state non-radiative processes (k_{nr}) in the micellar phase compared to bulk water [28].

The results obtained in the presence of silver sols are highly interesting. On adding microliter amounts of surfactant-stabilized silver sols to the TX-incorporated fluorophore, quenching of the latter's fluorescence is observed (Table 3). The results have been reported for a maximum silver sol concentration of 1.1×10^{-4} M. The limit on the maximum concentration is imposed by the fact that the

Table 3
Results of fluorescence studies[a]

System studied	[AgX] in mol l^{-1}	λ_{max}^{em} (nm)	ϕ_f^*	K_s (M^{-1})	k_q (M^{-1} s^{-1})
1-AN in aq. TX-100	–	440	0.60 (ϕ_f^0)	–	–
Green sol (PC) prepared from $AgNO_3$	1.1×10^{-4}	448	0.25	1.2×10^4	6.0×10^{11}
Yellow sol (PC) prepared from $AgNO_3$	1.1×10^{-4}	435	0.35	6.7×10^3	3.3×10^{11}
Yellow sol (C) prepared from $AgNO_3$	1.1×10^{-4}	448	0.30	8.2×10^3	4.1×10^{11}
Green sol (PC) prepared from Ag_2SO_4	1.1×10^{-4}	449	0.15	2.8×10^4	13.8×10^{11}
$AgNO_3$ solution	1.1×10^{-4}	443	0.40	4.5×10^4	2.7×10^{11}

[a] PC — photochemically prepared; C — chemically prepared; ϕ_f^0 — quantum yield of 2.5×10^{-5} M 1-AN in aqueous TX-100 (4×10^{-3} M); ϕ_f^* — absolute quantum yields determined using quinine sulfate in 0.5N H_2SO_4 as standard (ϕ_f=0.55); τ_f^0=20.3 ns, lifetime of 2.5×10^{-5} M 1-AN in aq. TX-100 (4×10^{-3} M).

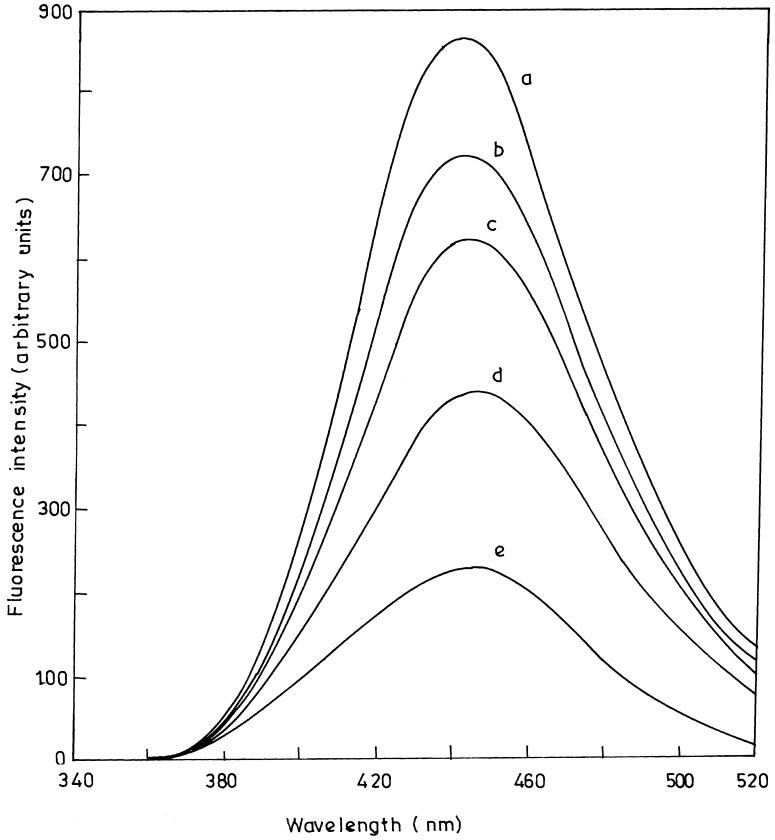

Fig. 7. Effect of the green silver sol prepared photochemically from Ag_2SO_4 on the fluorescence of 2.5×10^{-5} M 1-AN in 4×10^{-3} M aqueous TX-100, [Ag_2SO_4] being: (a) 0 M; (b) 1.3×10^{-5} M; (c) 2.7×10^{-5} M; (d) 5.3×10^{-5} M; (e) 1.1×10^{-4} M.

yellow sol is formed at a much lower concentration of Ag (I) compared to the concentration required for formation of the green sol. Comparison of the quenching results necessitates use of the same final silver concentration and to maintain a final concentration greater than 1.1×10^{-4} M, a large volume of yellow sol is required. This may introduce errors due to dilution effect. Hence a reasonable concentration of 1.1×10^{-4} M is maintained for comparative study. It is found that the fluorescence of TX-incorporated 1-AN is quenched to the maximum extent by the green sol prepared photochemically from Ag_2SO_4 (Fig. 7 and Table 3). Next is the green sol prepared photochemically from $AgNO_3$. The yellow sol prepared photochemically from $AgNO_3$ has the weakest quenching ability.

The above results may be explained as follows. In order to ascertain the cause for sol-induced quenching, first the extent of quenching due to the commonly encountered heavy atom effect was determined. There exists a possibility that the fluorescence quenching of 1-AN may be caused by the trace Ag (I) generated by aerial oxidation [25]. On addition of 1.1×10^{-4} M $AgNO_3$, the fluorescence was quenched by only 33% (Table 3) which cannot account for the almost 75% quenching caused by the same concentration of Ag sols. Thus, keeping in mind the fact that in aqueous Ag sol, the concentration of free Ag (I) is much lower than that of Ag sol, it can be concluded that the contribution of heavy atom-induced quenching is almost negligible compared to that caused by Ag sols [25]. The model proposed by Weitz et al. attempts to explain the sol particle-induced fluorescence quenching [23,24]. The excitation of the electronic plasma resonance leads to an increased absorption rate. Again, the molecular emission dipole excites the plasma resonance leading to an increase in the rate of radiative decay. However, the non-radiative branch of the decay provides an additional damping effect. When the latter overwhelms the other two processes, quenching of fluorescence is observed.

The next issue to be addressed is the nature of quenching, that is whether it is a case of dynamic or static quenching. Ag sols absorb very insignificant amount of light at the exciting wavelength. Therefore, the quenching is not due to absorption of light by Ag sols. Here, concentration quenching by dipolar energy transfer between the fluorophore molecules is not considered since the ratio of Ag sol concentration to probe concentration being ~4. The probability of fluorophore molecules crowding together is less. Moreover, if concentration quenching were to occur, then with increasing Ag sol concentrations efficiency of quenching would decrease, thus leading to an increase in ϕ_f. However, this is not observed. Now, for both static and dynamic quenching, the fluorophore and quencher must be in contact. For dynamic quenching, the quencher must diffuse to the fluorophore or

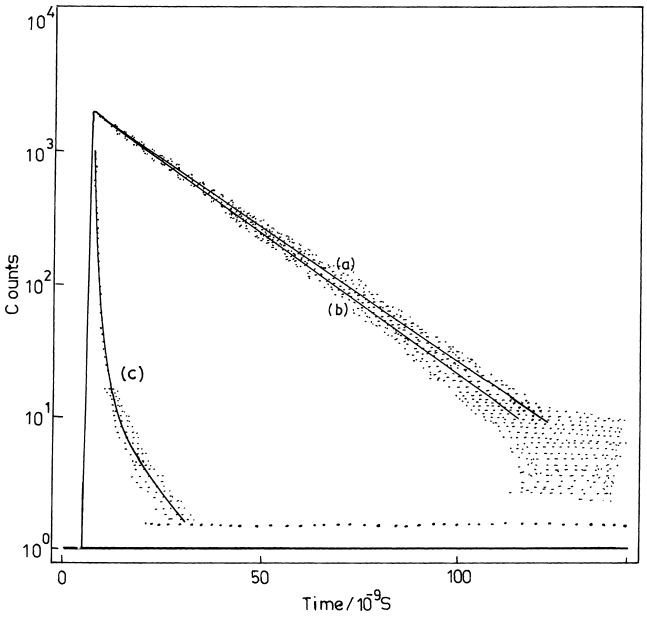

Fig. 8. Emission decay of 2.5×10^{-5} M 1-AN in: (a) 4×10^{-3} M aqueous TX-100; (b) (a) $+1.1\times10^{-4}$ M green silver sol and (c) decay of the exciting pulse, that is nitrogen lamp.

vice versa within the lifetime (τ) of the excited state. Assuming that the diffusion coefficient (D) of 1-AN is similar to that of other organic molecules in water ($0.05\,\text{Å}^2\,\text{ps}^{-1}$) [39], the mean square distance of diffusion $(\Delta x^2)=2D\tau$ [40]. Thus, the 1-AN molecule can diffuse about $45\,\text{Å}\,\text{ns}^{-1}$ and within its lifetime of 20.3 ns, when bound to TX-100, 1-AN scans a region of radius of a few nanometer. Thus, it can come into contact with the quencher, that is Ag sol (diameter<6 nm). However, if dynamic quenching were to occur, then the ratio of ϕ_f of 1-AN in absence of quencher to that in its presence (τ_f^0/τ_f) would correspond to an equal change in its lifetime (τ_f^0/τ_f) [40]. However, such a correspondence is not observed in the present case. Lifetime measurements reveal practically no change in τ_f of 2.5×10^{-5} M 1-AN in 4×10^{-3} M aqueous TX-100, on addition of Ag sols. The lifetime in aqueous micelle, that is τ_f^0 (20.3 ns) decreases only very slightly to 19.2 ns in the presence of Ag sols (Fig. 8). This nominal decrease is within an error limit of ±1.0 ns. Thus, quenching by Ag sols in this work is a case of static quenching. Static quenching removes a fraction of the fluorophore from observation. The complexed fluorophores are non-fluorescent and the only observed fluorescence is from the uncomplexed fluorophore, which is unperturbed and hence lifetime is unaffected.

Static fluorescence quenching usually results from the formation of a non-fluorescent complex between the fluorophore and the quencher [40]. The formation of a ground state complex alters the absorption spectrum of the probe. In this work, the silver plasmon band (shape and height) was affected slightly by addition of the probe implying chemisorption of 1-AN onto the sol surface [21,25]. Thus, some sort of ground-state complex is formed between 1-AN and the Ag sol, which on excitation absorbs light and immediately returns to the ground state without emitting a photon.

The dependence of the fluorescence intensity upon the quencher concentration is plotted and linear plots are obtained for all types of sols. This indicates that only one type of quenching, that is static quenching occurs. For static quenching, the dependence of ϕ_f^0/ϕ_f on quencher concentration [Q] is similar to that for dynamic quenching except that the quenching constant in the plot is now the association constant K_s [40]. Static quenching of 1-AN by all types of Ag sols obeys a linear relation (Fig. 9), Eq. (2). This linearity (standard deviation $\pm0.89\%$, average of five determinations) is indicative of a single class of fluorophores, all equally accessible to the quencher.

$$\frac{\phi_f^0}{\phi_f} = 1 + K_s[Q] \tag{2}$$

$\phi_f{}^0$=quantum yield in absence of quencher; ϕ_f=quantum yield in presence of quencher; [Q] in Fig. 9 represents the total quencher concentration.

K_s is the association constant for complex formation.

Table 3 lists the K_s values for the different sols. The green sol prepared photochemically from Ag_2SO_4 forms the strongest complex with 1-AN, that is, $K_s=28013\,\text{M}^{-1}$, while the yellow sol formed photochemically from $AgNO_3$ forms the weakest complex, $K_s=6675\,\text{M}^{-1}$. The binding of 1-AN to Ag sols can be explained by the strong affinity of Ag for nitrogen as evident from SERS studies [9,31]. $SO_4{}^{2-}$ being larger in size than $NO_3{}^-$, produces a larger squeezing effect, thus bringing 1-AN and Ag sol in closer contact. Hence the higher value of K_s for the sol prepared from Ag_2SO_4 compared to that prepared from $AgNO_3$.

A careful study of Table 3 reveals that the strength of association of the Ag sol to 1-AN can be directly linked to its efficiency as a quencher. The more strong is the fluorophore complexed to the Ag sol (i.e. high K_s), the larger is the extent of static quenching (i.e. high ϕ_f^0/ϕ_f). Considering the lifetime of 1-AN in the absence of quencher (τ_o=20.3 ns), the 'apparent bimolecular quenching constant' k_q, can be calculated from K_s (Table 3). The values of k_q so obtained range from 2.7×10^{11} to $13.8\times10^{11}\,\text{M}^{-1}\,\text{s}^{-1}$. These values are larger than those possible for a diffusion-controlled reaction [40]. A k_q value of $1\times10^{10}\,\text{M}^{-1}\,\text{s}^{-1}$ is the largest possible value in aqueous solutions [40]. This fact further strengthens the contention that complex formation between 1-AN and Ag sol is the cause for the quenching rather than any dynamic diffusion process.

Addition of almost all types of Ag sols to 1-AN in aqueous TX-100 is accompanied by a red shift in the emission maxima (λ_{em}^{max}) from 440 to 447–449 nm. λ_{em}^{max} of 1-AN in neat water is reported to be 455 nm [27]. The red shift in the presence of Ag sols with respect to aqueous TX, that is 440 nm shows that 1-AN experiences a more polar environment in the presence of sols [27,28]. 1-AN, having an apolar naphthalene moiety is probably located near the surface of

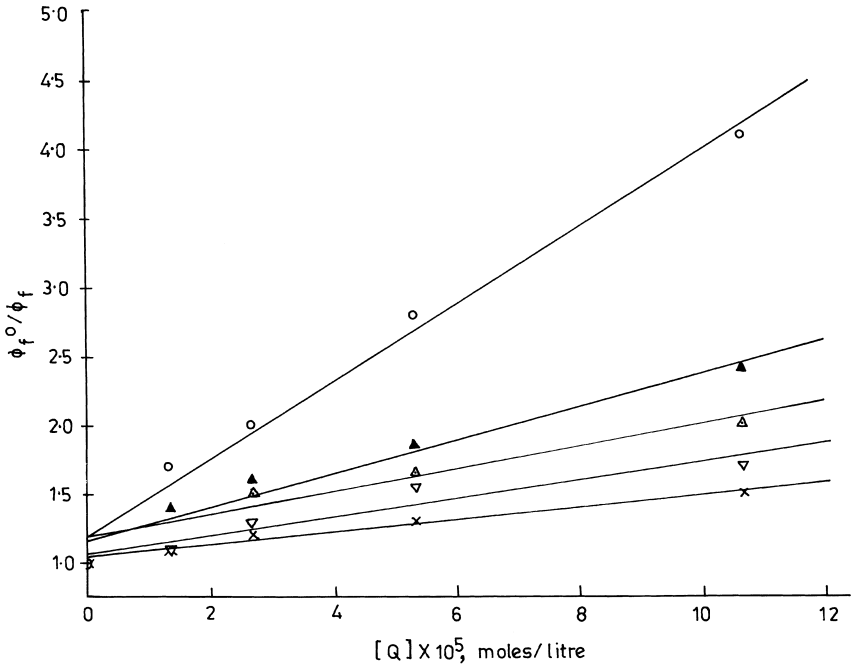

Fig. 9. Linear plots for the quenching of fluorescence of 2.5×10^{-5} M 1-AN in 4×10^{-3} M aqueous TX-100 by silver sols and Ag (I): (a) green sol from $AgNO_3$ (▲); (b) photochemically prepared yellow sol from $AgNO_3$ (▽); (c) chemically prepared yellow sol from $AgNO_3$ (△); (d) photochemically prepared green sol from Ag_2SO_4 (○) and (f) $AgNO_3$ solution (×).

the micellar interior. On complex formation with the Ag sol, the fluorophore is exposed to a more polar environment than the micellar interior but less polar than bulk water where λ_{em}^{max}=455 nm. This may be the Stern layer. For Ag (I) ion, the binding being weaker, the red shift is smaller. However, the photochemically prepared yellow sol presents a unique case where a 5 nm blue shift is observed. The cause for this anomalous behavior is not clearly understood. One reason may be that the smaller yellow sol particles may reside near the micellar palisade layer, thus forcing the fluorophore to move further into the micellar interior.

3.3. Surface-enhanced Raman scattering (SERS)

As SERS studies of pyridine in the presence of chemically prepared yellow Ag sol have already been reported [5,6,41,42], the photochemically prepared green silver sol was used for the SERS studies. The sol by itself showed only a few weak Raman bands, mostly near 1600 cm^{-1} which may be due to ascorbic acid (used as reduction sensitizer) or TX-100. However, with the addition of 4×10^{-2} M pyridine, enhanced bands at 1012 and 1039 cm^{-1} were seen. These bands were proved to be SERS bands of pyridine since they were not strongly polarized. Solution pyridine bands are strongly polarized and almost disappear in vertical polarization. Successive addition of an electrolyte, for example, KCl (2×10^{-4} M) enhances the pyridine bands 2.1 times (data not shown) while the 1600 cm^{-1} band remains unaffected. The salt KCl leads to enhanced aggregation of Ag sols to form the linear aggregates, thus a large enhancement in SERS signal is observed. The band at 250 cm^{-1} was due to adsorbed Cl^-. The SERS spectra of pyridine showed a much larger enhancement in the presence of the green sol compared to the pyridine spectra with yellow sol (dotted line in Fig. 10).

In case of silver and gold sols, existing evidence shows that aggregation is essential for high SERS activity [6]. It is known that the effect of close proximity of the spheres within the particle aggregates is to shift the plasma resonance to longer wavelengths due to coupling between the plasma modes of adjacent spheres [43]. Thus, the absorption spectrum is changed. Earlier works have shown that there is a similarity between the excitation profiles for SERS and the absorption spectra of aggregated Ag and Au sols [6]. For these sols, the plasma resonance of the aggregates were sharp and the SERS excitation profile was found to peak at a wavelength close to λ_{max}^{abs} [5,6]. Creighton et al. have also reported that aggregated or aspherical particles increase the absorption cross-section, thus increasing the surface intensity enhancements at the resonance wavelengths [6,8]. Siiman et al. have correlated SERS intensity to particle size and the state of aggregation of Ag colloids [44]. For aggregated spheres or larger particles, there are a hierarchy of higher order modes. Resonant excitation of one may give rise to strong fields localized inside the particle, thus giving rise to strong absorption, whereas resonant excitation of some other mode may cause strong fields localized just outside the particle surface giving rise to SERS [45]. Thus, linear aggregation of Ag in the green sol corroborates two presumptions — an additional absorption band (∼630 nm) and enhancement of SERS signal intensity.

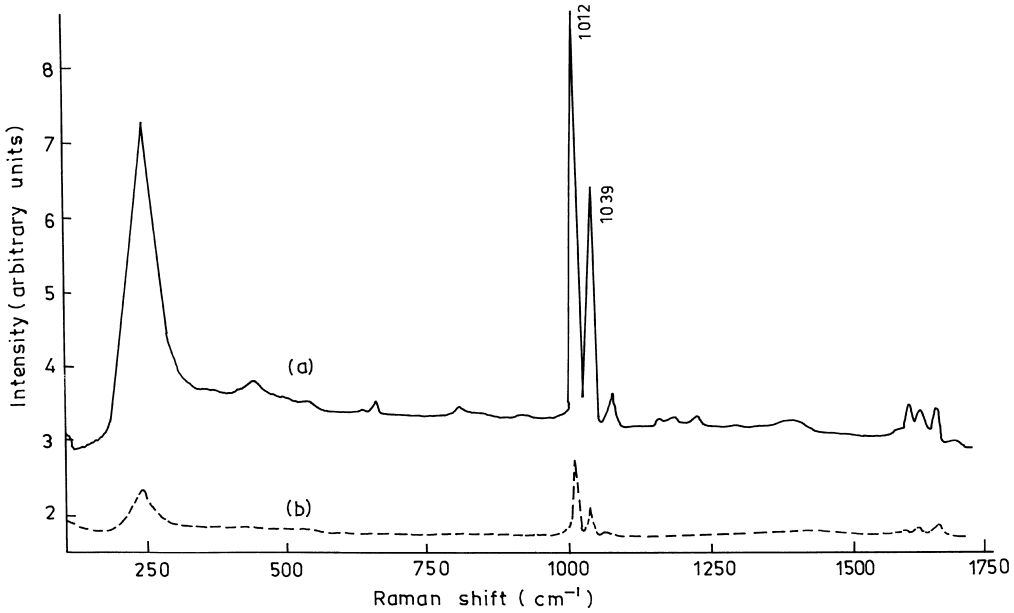

Fig. 10. SERS spectra of pyridine: (a) with the green silver sol prepared from $AgNO_3$, [$AgNO_3$]=1×10^{-3} M, [TX-100]=5×10^{-3} M, [AA]=8.5×10^{-5} M, [KCl]=2×10^{-4} M and (b) with yellow sol prepared under the same conditions as for the green sol but with [AA]=1×10^{-5} M.

4. Conclusion

One novel aspect of this work is the effect of anions of precursor salts on the efficiency of photochemical reduction of Ag (I) to Ag (0). In this respect, the SO_4^{2-} ion has been found to be the most efficient. Another highlight of this work is the realization of the fact that when individual spherical yellow Ag sols aggregate in a linear fashion, their efficiency in fluorescence quenching increases along with an enhancement of SERS activity. Apart from these highly interesting observations, this work reports on the preparation and properties of photochemically prepared silver sol. The stability and reproducibility of the photochemically-prepared green sol is far better than that produced chemically. Another importance of this work is the action of UV light in inducing symmetric aggregation, which is very difficult to achieve by the action of chemicals. UV light induced cleavage of ascorbic acid to produce radical species is believed to be responsible for the reduction for Ag (I). The formation of green silver sol requires a delicate balancing of ascorbic acid and precursor silver salt concentrations. A necessary requirement for green sol formation is the presence of 1:1 TX-100 aqueous medium. However, in the water pools of TX-100 reverse micelle, only the yellow sol is formed. Fluorescence studies were carried out in order to delve further into the structure and nature of Ag sols. Fluorescence quenching studies show that SO_4^{2-} ions most favor the formation of linearly aggregated Ag sol. Now, fluorescence and Raman effect are both examples of inelastic scattering by molecules. To a first approximation, the molecule is akin to a polarizable dipole, which is excited at one frequency and reemits at a shifted frequency [45]. An effort is thus made to correlate the SERS and fluorescence results obtained with the Ag sols. Often, the enhancement of selective vibrations in SERS can be explained on the basis of a charge-transfer model which involves interaction between the adsorbed molecules and the metal surface [42,46,47]. Another explanation for the charge transfer may come from the fact that the incident photon may excite an electron from the metal to an unoccupied state of the molecule or vice versa. In either case, there is an interaction between the adsorbate and adsorbent. The interaction may be chemical or electronic. The fluorescence quenching results in this report have been explained on the basis of a ground-state complex formation between the fluorophore and the Ag sol. This, too involves some interaction between the two. Thus, there seems to be some indirect correlation between fluorescence quenching by silver sols and the consequent SERS enhancement by them. These results can be compared to those obtained by Weitz et al [23,24]. This result has important implications in the study of dyes or biological molecules. Normally, resonance Raman scattering (RRS) is a weak process and is often obscured by fluorescence for molecules with high ϕ_f. This work holds prospects for enhancing RRS for highly fluorescent molecules (e.g. 1-AN) using linear aggregates of Ag.

Acknowledgements

The authors wish to thank Prof. J. Belloni for helpful discussions. Thanks are due to Prof. J.A. Creighton for his help with the SERS studies and for useful suggestions. Prof. S.P. Moulik is thanked for letting the authors use the dynamic light scattering apparatus. Dr. S. Basak is acknowledged for his generosity in letting the authors perform the lifetime studies in his laboratory.

References

[1] H. Haberland, Clusters of Atoms and Molecules, Vol. 2, Springer, Berlin, 1994.
[2] U. Kriebig, M. Vollmer, Optical Properties of Metal Clusters, Springer, Berlin, 1995.
[3] M. Quinten, D. Schönauer, U. Kriebig, Z. Phys. D 12 (1989) 521.
[4] U. Kriebig, Z. Phys. D 3 (1986) 239.
[5] J.A. Creighton, C.G. Blatchford, M.C. Albrecht, J. Chem. Soc. Faraday Trans. 2 (75) (1979) 790.
[6] C.G. Blatchford, J.R. Campbell, J.A. Creighton, Surf. Sci. 120 (1982) 435.
[7] J.A. Creighton, M.S. Alvarez, D.A. Weitz, S. Garoff, M.W. Kim, J. Phys. Chem. 87 (1983) 479.
[8] J.A. Creighton, D.G. Eadon, J. Chem. Soc. Faraday Trans. 87 (1991) 3881.
[9] M.G. Albrecht, J.A. Creighton, J. Am. Chem. Soc. 99 (1977) 5215.
[10] G. Mie, Ann. Phys. 25 (1908) 377.
[11] M. Mostafavi, J.L. Marignier, J. Amblard, J. Belloni, Radiat. Phys. Chem. 34 (1989) 605.
[12] M. Mostafavi, N. Keghouche, M.-O. Delcourt, Chem. Phys. Lett. 169 (1990) 81.
[13] M. Kerker, The Scattering of Light and Other Electromagnetic Radiation, Academic Press, New York, 1969, p. 38.
[14] J.I. Gersten, A. Nitzan, in: R.K. Chang, T.E. Furtak (Ed.), Surface-Enhanced Raman Scattering, Plenum Press, New York, 1982, p. 89.
[15] N. Liver, A. Nitzan, J.I. Gersten, Chem. Phys. Lett. 111 (1984) 449.
[16] C.G. Blatchford, O. Siiman, M. Kerker, J. Phys. Chem. 87 (1983) 2503.
[17] D.C. Skillman, C.R. Berry, J. Chem. Phys. 48 (1968) 3297.
[18] A. Henglein, P. Mulvaney, T. Linnert, Faraday Discuss. 92 (1991) 31.
[19] P. Mulvaney, A. Henglein, J. Phys. Chem. 94 (1990) 4182.
[20] A. Henglein, T. Linnert, P. Mulvaney, Ber. Bunsen-Ges. Phys. Chem. 94 (1990) 1449.
[21] T. Linnert, P. Mulvaney, A. Henglein, J. Phys. Chem. 97 (1993) 679.
[22] T. Linnert, P. Mulvaney, A. Henglein, Ber. Bunsen-Ges. Phys. Chem. 95 (1991) 838.
[23] D.A. Weitz, S. Garoff, J.I. Gersten, A. Nitzan, J. Chem. Phys. 78 (1983) 5324.
[24] D.A. Weitz, S. Garoff, C.D. Hanson, T.J. Gramila, J.I. Gersten, J. Lumin. 24/25 (1981) 83.
[25] L. Zang, C.-Y. Liu, X.-M. Rem, J. Chem. Soc. Chem. Commun. (1995) 447.
[26] M. Tata, S. Banerjee, V.T. John, Y. Waguespack, G.L. McPherson, Coll. Surf. A-Physicochem. Eng. Aspects 127 (1997) 39.
[27] S.R. Meech, D.V. O'Connor, D. Phillips, A.G. Lee, J. Chem. Soc. Faraday Trans. 79 (1983) 1563.
[28] R.S. Sarpal, S.K. Dogra, J. Chem. Soc. Faraday Trans. 88 (1992) 2725.
[29] T. Pal, N.R. Jana, T. Sau, Radiat. Phys. Chem. 49 (1997) 127.
[30] J.I. Gersten, A. Nitzan, J. Chem. Phys. 73 (1980) 3023.
[31] M. Fleischmann, P.J. Hendra, A. McQuillan, J. Chem. Phys. Lett. 28 (1974) 163.
[32] C. Kumar, D. Balasubramanian, J. Coll. Int. Sci. 69 (1979) 271.
[33] S. Subramanian, J.M. Nedeljkovic, R.C. Patel, J. Coll. Int. Sci. 150 (1992) 81.
[34] B.G. Ershov, Russ. Chem. Rev. 50 (1981) 2137.
[35] P.V. Kamat, M. Flumiani, G.V. Hartland, J. Phys. Chem. 102B (1998) 3123.
[36] M. Fedurco, V. Shklover, J. Augustynski, J. Phys. Chem. 101B (1997) 5158.
[37] A.L. Rogach, G.P. Schevchenko, Z.M. Afanas'eva, V.V. Sviridov, J. Phys. Chem. 101B (1997) 8129.
[38] C. Petit, P. Lixon, M.-P. Pileni, J. Phys. Chem. 97 (1993) 12974.
[39] C.B. Cho, M. Chung, J. Lee, T. Nguyen, S. Singh, M. Vedamuthu, S. Yao, J.-B. Zhu, G.W. Robinson, J. Phys. Chem. 99 (1995) 7806.
[40] J.R. Lakowicz, Principles of Fluorescence Spectroscopy, Plenum Press, New York, 1983, (Chapter 9).
[41] U.K. Sarkar, A.J. Pal, S. Chakrabarti, T.N. Misra, Chem. Phys. Lett. 190 (1992) 59.
[42] R. Clippe, R. Evrard, A.A. Lucas, Phys. Rev. B 14 (1976) 1715.
[43] O. Siiman, L.A. Bunn, R. Callaghan, C.G. Blatchford, M. Kerker, J. Phys. Chem. 87 (1983)
[44] J.F. Owen, R.K. Chang, P.W. Barber, Opt. Lett. 6 (1981) 540.
[45] M. Kerker, Acc. Chem. Res. 17 (1984) 271.
[46] A. Kudelski, P.J. Bukowska, Chem. Phys. Lett. 222 (1994) 555.
[47] B. Chase, B. Parkinson, J. Phys. Chem. 95 (1991) 7810.